IJARSCT
International Journal of Advanced Research in Science, Communication and Technology
International Open-Access, Double-Blind, Peer-Reviewed, Refereed, Multidisciplinary Online Journal
ISSN: 2581-9429
Volume 6, Issue 7, April 2026
Impact Factor: 8.2

Investigation of Electrical Properties of Aluminium Dopped Calcium Hexaferrites for Microwave Devices

Vasudha T. Thawari*[1], Sanjay R. Gawali
[1*]Department of Physics, Dr. Ambedkar College, Chandrapur, (M.S.), India
*Corresponding author's e-mail: thevasudhathawari@gmail.com

Abstract: *A series of aluminium-substituted calcium hexaferrites with compositions $CaAl_xFe_{12-x}O_{19}$ (x = 0, 1, 3, and 5) were synthesized by microwave assisted sol-gel auto-combustion route. The structural characteristics of the prepared samples were investigated using X-ray diffraction (XRD) analysis, which confirmed the formation of a single-phase M-type hexagonal ferrite structure. The lattice parameters a and c, unit cell volume V, X-ray density ρ_x, and bulk density ρB were observed to decrease with increasing aluminium substitution, whereas the porosity P increased with higher Al content. DC electrical conductivity measurements were performed in the temperature range of 300–800 K using an impedance analyzer. The conduction mechanism was interpreted in terms of the Verwey hopping model. An increase in electrical resistivity was noted with the substitution of Al^{3+} ions for Fe^{3+} ions, indicating the material's suitability for microwave device applications. Furthermore, the drift mobility was found to increase with higher aluminium concentration in the calcium hexaferrite system.*

Keywords: M-type hexagonal ferrite, structural property, electrical property, drift mobility, sol-gel auto-combustion route, TEM, etc.

I. INTRODUCTION

Ferrites are broadly classified into three main families: spinel, hexagonal, and garnet ferrites. Among these, M-type strontium hexaferrite (SrFe□□O□□) has been extensively investigated over the years due to its significant scientific and technological importance [1]. Owing to its excellent thermal stability, high chemical durability, corrosion resistance, and distinctive magnetic and electrical characteristics, strontium hexaferrite is widely employed in recording media, telecommunication systems, magneto-optical devices, and microwave applications [2,3]. Its high electrical resistivity and low eddy current losses make it suitable for applications spanning microwave to radio-frequency ranges. Additionally, this material is commonly used in loudspeakers, permanent magnet motors, various coil-based instruments such as galvanometers, voltmeters, and ammeters, as well as microphones. Compared to other permanent magnetic materials, hexaferrites offer the advantages of lower cost and higher operational efficiency.

A survey of the literature indicates that hexaferrites can be synthesized using a variety of techniques. These include the hydrothermal method [4], solid-state reaction route [5], sol–gel process [6,7], microwave-assisted synthesis [8], and the co-precipitation method [9], combustion [10,11].

In the present work, M-type aluminium-substituted calcium hexaferrite was synthesized using a microwave-induced sol–gel auto-combustion technique. This approach is a simple, safe, and rapid method that facilitates the formation of ultrafine powders while significantly reducing processing time. Its key advantages include high chemical homogeneity, high phase purity, and the production of nanosized particles. Moreover, the sol–gel auto-combustion route yields ultrafine nanopowders with a narrow particle size distribution, excellent compositional uniformity, and a higher likelihood of single-domain structure formation [12,13]. Additionally, efforts were made to enhance the microstructure, electrical conductivity, and drift mobility of aluminium-substituted calcium hexaferrite.

DOI: 10.48175/IJARSCT-33022

IJARSCT
International Journal of Advanced Research in Science, Communication and Technology
International Open-Access, Double-Blind, Peer-Reviewed, Refereed, Multidisciplinary Online Journal
ISSN: 2581-9429
Volume 6, Issue 7, April 2026
Impact Factor: 8.2

II. EXPERIMENTAL

2.1. Sample preparations

The series of aluminium dopped calcium hexaferrites was prepared by Sol–gel auto-combustion route. Sol–gel auto-combustion route is a unique combination of self propagating chemical sol–gel method and combustion route.

In this method, the metal nitrates acts as an oxidizing reactant and fuel urea as a reducing reactant. Stoichiometric quantities of analytical-reagent-grade metal nitrates such as Ca(NO□)□·4H□O, Fe(NO□)□·9H□O, Al(NO□)□·9H□O, and the fuel CO(NH□)□ were dissolved in a minimum amount of hot distilled water. The prepared solution was then placed on a magnetic stirrer to obtain the homogeneous solution. This homogeneous solution was then placed in a microwave oven. At first, the solution boiled and underwent dehydration, followed by thermal decomposition accompanied by the release of a large volume of gases such as N□, NH□, and HNCO during the combustion process. Once spontaneous ignition occurred, the mixture burned vigorously, generating a large amount of heat that rapidly evaporated the solvent and resulted in the formation of a solid product at temperatures exceeding 1000 °C. The combustion yielded voluminous brown ash, which was subsequently ground using an agate mortar to obtain fine calcium hexaferrite powder.

A few drops (2–3) of a 10% polyvinyl alcohol (PVA) solution were added to the powder and mixed thoroughly before pelletization. The mixture was pressed into pellets of 15 mm diameter and 5–8 mm thickness using a stainless-steel die under appropriate uniaxial pressure for 5 minutes. Polyvinyl acetate was used as a binder. The pellets were then calcined at 800 °C for 2 hours in an electric furnace to obtain M-type calcium hexaferrite samples. For electrical measurements, both surfaces of the pellets were coated with silver paste to ensure good electrical contact. Figure 1 (a) shows peak reaction stage in microwave oven and (b) shows ash obtained after combustion.

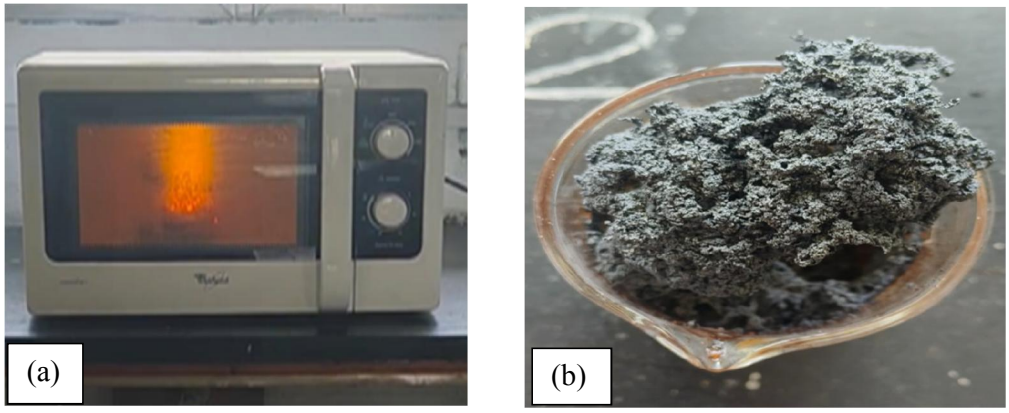

Figure 1(a) : Peak reaction stage in microwave oven (b)Ash obtained after combustion.

2.2 Characterization

The crystalline phases of the prepared samples were analyzed using a Philips Holland X-ray diffractometer (Model PW 1710). Cu Kα radiation with a wavelength of 1.54056 Å was employed for the XRD measurements. The lattice constants a and c, unit cell volume (V), X-ray density (ρ_x), bulk density (ρ_B),and porosity (P) were determined using standard crystallographic relations. The interplanar spacing (d) is related to the Miller indices (h, k, l) and lattice parameters (a and c) by the following equation:

$$\frac{1}{d^2} = \frac{4(h^2+hk+k^2)}{3a^2} + \frac{l^2}{c^2} \quad \text{..... (1)}$$

The unit cell volume was calculated using the relation: $V=0.8666a^2c$ ..... (2)

The X-ray density (ρ_x), was calculated using the relation:

$$\rho_X = \frac{ZM}{NV} \quad \text{..... (3)}$$

IJARSCT
International Journal of Advanced Research in Science, Communication and Technology
International Open-Access, Double-Blind, Peer-Reviewed, Refereed, Multidisciplinary Online Journal
ISSN: 2581-9429 Volume 6, Issue 7, April 2026 Impact Factor: 8.2

where Z represents the number of formula units per unit cell, which is equal to 2 for M-type hexaferrites, M is the molecular weight, N denotes Avogadro's number, and V is the unit cell volume.

The bulk density (ρ_B) of the pellets was determined from the following expression:

$$\rho_B = \frac{m}{(\pi r^2)h} \quad \text{..... (4)}$$

where m is the mass of the cylindrical pellet, r is the radius of the pellet, and h is the thickness (height) of the pellet.

The porosity (P)was evaluated using the relationship:

$$P = 1 - \frac{\rho_B}{\rho_X} \quad \text{.....(5)}$$

where ρ_B is the bulk density and ρ_X is the X-ray density.

The DC electrical resistivity of the ferrite system was measured using the four-probe technique over the temperature range of 300–800 K. It was observed that the resistivity of all samples decreases with increasing temperature, indicating semiconducting behavior and following the Arrhenius relation

$$\rho = \rho_0 \exp\left(\frac{\Delta E}{k_B T}\right) \quad \text{.....(6)}$$

Where, 'k_B' is the Boltzmann constant, 'T' represents the absolute temperature, and 'ΔE ' is the activation energy. The activation energy corresponds to the energy required for charge carriers to hop between neighboring ions, thereby contributing to electrical conduction.

The activation energy of aluminium-substituted calcium hexaferrites was evaluated from the slope of the plots of ln(ρ) versus 1000/T, both above and below the transition temperature (T□). The drift mobility (μ_d) of all the synthesized hexaferrite samples was determined using the relation:

$$\mu_d = 1/ne\rho \quad \text{..... (7)}$$

where e represents the electronic charge, ρ is the DC electrical resistivity at a given temperature, and n is the charge carrier concentration.

The carrier concentration was calculated using the expression:

$$n = \frac{N_A \rho_m P_{Fe}}{M} \quad \text{..... (8)}$$

where N_a denotes Avogadro's number, ρ is the bulk density, M is the molecular weight of the sample, and P_{Fe} represents the number of iron atoms in the chemical formula.

III. RESULTS AND DISCUSSION

3.1. XRD analysis

Figure 2 reveals that the X-ray diffractograms of $CaAl_xFe_{12-x}O_{19}$ (x=0, 1, 3 and 5) samples.

The XRD data of the prepared samples were analyzed using computer software such as PCPDFWIN, Powder-X, and the FullProf software suite. The diffraction patterns were compared with standard JCPDS data to identify the phases present in the samples. It was observed that all the diffraction peaks correspond well with the standard pattern, and no additional peaks were detected. This confirms the formation of a single-phase magnetoplumbite structure in the synthesized samples. The space group of the samples was identified as $P6_3/mmc$ (No. 194).

IJARSCT
International Journal of Advanced Research in Science, Communication and Technology
International Open-Access, Double-Blind, Peer-Reviewed, Refereed, Multidisciplinary Online Journal
ISSN: 2581-9429
Volume 6, Issue 7, April 2026
Impact Factor: 8.2

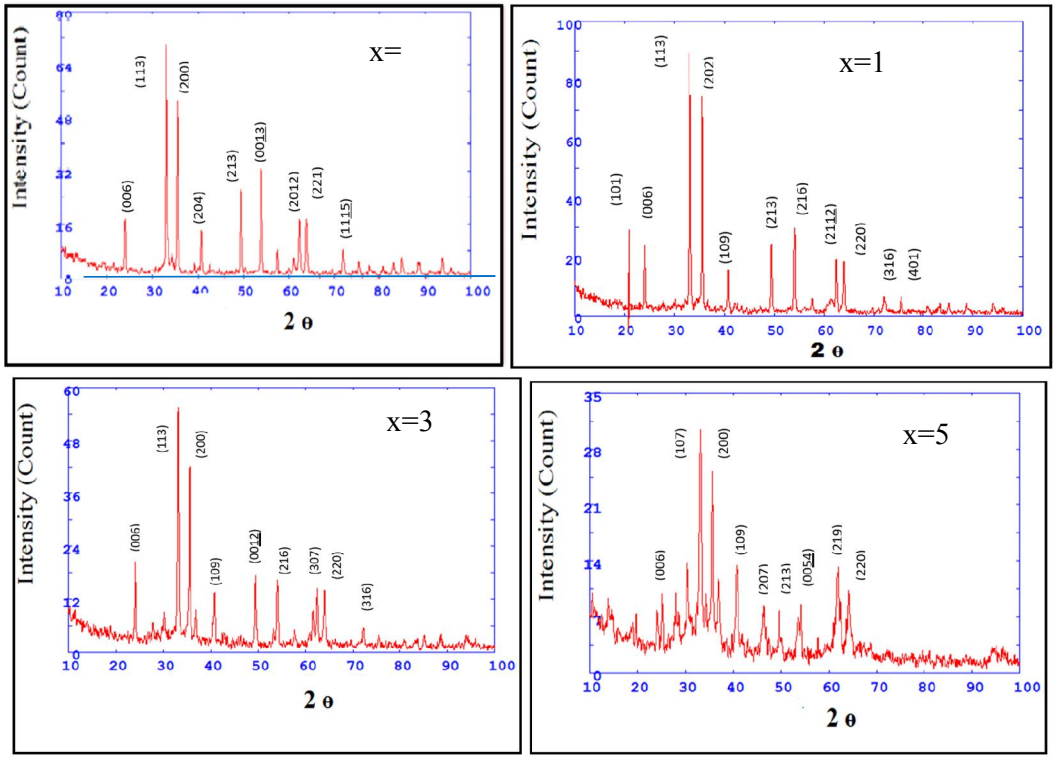

Figure 2: XRD patterns of $CaAl_xFe_{12-x}O_{19}$ samples where x=0, 1, 3 and 5.

Lattice parameters (a & c), unit cell volume (V), X-ray density (ρ_X), bulk density (ρ_B) and porosity (P) of samples were calculated from XRD data and their values are enumerated in Table 1.

The lattice parameters a and c were found to decrease with increasing Al^{3+} ion concentration [14], as illustrated in Table 1. This reduction is attributed to the smaller ionic radius of Al^{3+} ions (0.53 Å) compared to that of Fe^{3+} ions (0.64 Å) in sixfold coordination. Consequently, the substitution of Al^{3+} ions leads to a contraction of the crystal lattice, resulting in a decrease in the unit cell volume of calcium hexaferrite [15-17].

3.2 Electrical Conductivity of samples

The electrical resistivity of the samples with concentration x of Al^{3+} ions at room temperature increases from 18.8 to 24.4 MΩ-m. There may be several factors for such increase in resistivity including the formation of other secondary phases and increases in porosity of the samples. The increase in porosity causes the separation between the grains. This separation may lead to difficulty in the conduction of the free electrons from grain to grain. The increase in resistivity may be due to the fact that Al^{3+} is more resistive than Fe^{3+} ions [19].

Table 1: Structural parameters of $CaAl_xFe_{12-x}O_{19}$ Samples where x=0, 1, 3 and 5.

Structural Parameters	x=0	x=1	x=3	x=5
Lattice parameter (a) in (Å)	5.8293	5.8240	5.8134	5.8041
Lattice parameter (c) in (Å)	22.1652	22.1520	22.1195	22.0898
Unit cell volume (V) in $(Å)^3$	652.262	650.689	647.376	644.436
X-ray density (ρ_X) in (gm/cm^3)	5.162	5.029	4.734	4.477
Bulk density (ρ_B) in (gm/cm^3)	2.884	2.791	2.582	2.326
Porosity (P) in (%)	44.621	45.45	47.07	48.47
Room Temperature Resistivity ρ	18.8	19.8	22.0	24.4

IJARSCT
International Journal of Advanced Research in Science, Communication and Technology
International Open-Access, Double-Blind, Peer-Reviewed, Refereed, Multidisciplinary Online Journal
ISSN: 2581-9429 Volume 6, Issue 7, April 2026 Impact Factor: 8.2

(MΩ-cm)					
Activation Energy ΔE (eV)	Ferri	0.12	0.14	0.72	0.18
	Para	1.58	1.51	1.18	1.64
Transition Temp T_t(K)		673	613	553	522

Figure 3 shows the graph of electrical conductivity ln(σ) verses temperature (10^3/T) for all ferrite samples. It has been seen from the figures that the value of ln(σ) decreases almost linearly with increasing reciprocal temperature upto transition temperature (T_t), where there is a slight change in slope occur in the plots. The temperature where kink is observed for the different composition of Al^{3+} ions in calcium hexaferrites is reported in Table 1. It can be seen from the table that the transition temperature T_t at which the kink in the plot of *l*n(σ) versus 10^3/T was observed are in the neighborhood of its Curie temperature. This reveals that the kink observed in the aluminium substituted calcium hexaferrite can be attributed to the order to disorder transitions. The graph plotted for ln(σ) vs (1000/T) shows a linear behavior [18]. The transition temperature T_t of synthesized samples varies in the range 522 to 673 K.

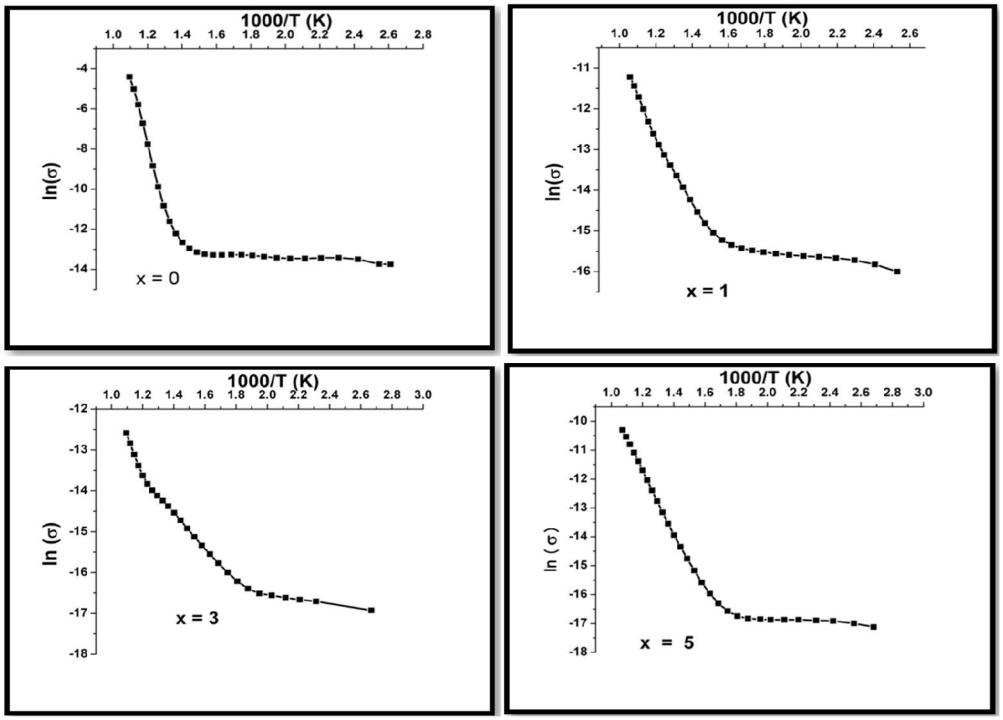

Figure 3: Variation of electrical conductivity ln(σ) verses temperature (10^3/T) for all ferrite samples

By increasing temperature, the conductivity of ferrite increases, indicating that these ferrites have semiconductors like behavior [20, 21]. The conduction in ferrite at room temperature is due to the impurities, where as at high temperature it is due to polaron hopping [22]. According to Verwey, the electronic conduction in ferrite is mainly due to hopping of electrons between ions of the same element present in more than one valence state, distributed randomly over crystallographically different lattice sites. The M-type ferrite crystallizes in a hexagonal structure with 64 ions per unit cell on 11 different symmetry sites. The 24 Fe^{3+} atoms are distributed over five distinct sites: three octahedral sites (12k, 2a and $4f_2$), one tetrahedral site ($4f_1$) and one new type of interstitial site (2b) which is not found with spinel and is surrounded by five oxygen ions constituting a trigonal bipyramid. In the hexagonal structure two tetrahedral sites are adjacent to each other and for these two sites only one metal ion is available. This metal ion now occupies position halfway between them, amidst the three oxygen ions. The distance between two metal ions at octahedral site is smaller

DOI: 10.48175/IJARSCT-33022

IJARSCT
International Journal of Advanced Research in Science, Communication and Technology
International Open-Access, Double-Blind, Peer-Reviewed, Refereed, Multidisciplinary Online Journal
ISSN: 2581-9429 Volume 6, Issue 7, April 2026 Impact Factor: 8.2

than the distance between a metal ion at octahedral site and tetrahedral site. The electron hopping between tetrahedral and octahedral sites under normal condition has a very small probability compared with that for octahedral-octahedral hopping. Hopping between two tetrahedral sites does not exist for the simple reason that there are only Fe^{3+} ions at tetrahedral site and any Fe^{2+} ions formed during processing preferentially occupy octahedral sites only. The hopping probability depends upon the separation between ions involved and the activation energy [23]. So, at high temperature, the hopping between $Fe^{2+} \leftrightarrow Fe^{3+}$ is possible.

3.3 Drifty mobility of samples

Figure 4 shows the variation of drift mobility with the temperature for aluminium substituted calcium hexaferrite. The Al^{3+} ions substituted calcium hexaferrite samples show a curvature at a specific temperature i.e. the drift mobility increases with the increase in temperature and above the specific temperature (T_t), the drift mobility increases abruptly with increase in the temperature.

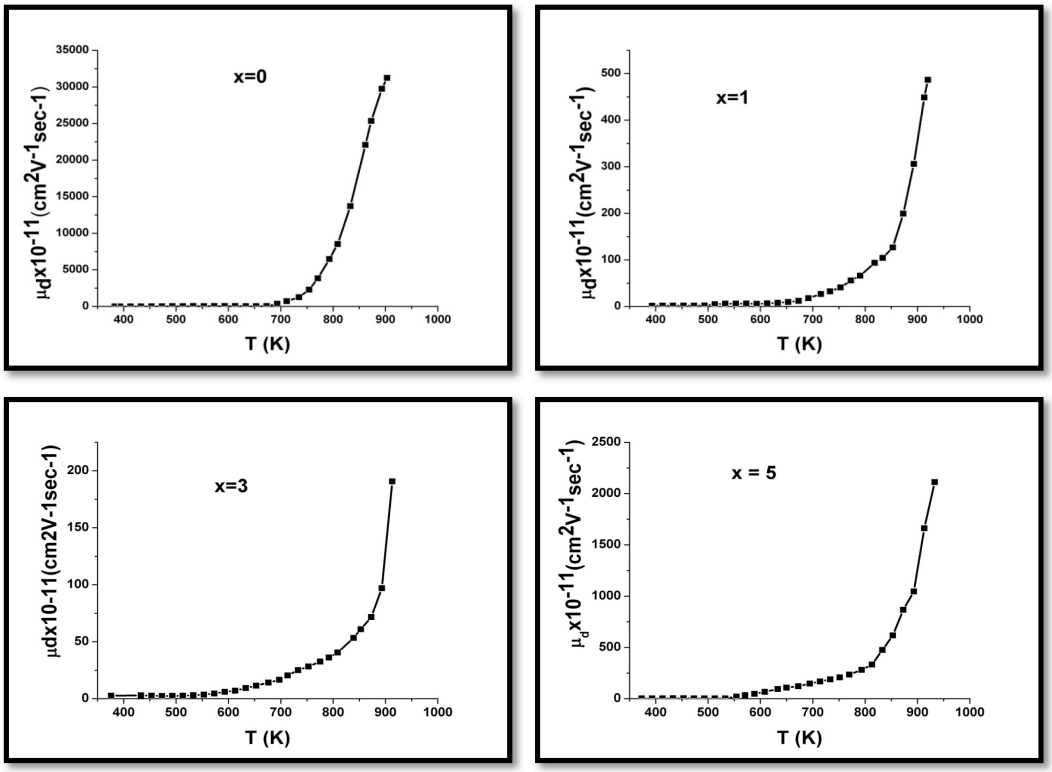

Figure 4 : Variation of drift mobility (μ_d) with temperature (T) of $CaAl_xFe_{12-x}O_{19}$ hexaferrite with x=0 to x=5.

The drift mobility of all the synthesized sample decreases with increasing amount of substituted Al. The decrease in drift mobility is due to increase in resistivity by doping Al^{3+} ions. The decrease in drift mobility with increasing amount of Pb in Sr hexaferrite [24]. The decrease in drift mobility with increasing substituent Al and Ga in strontium ferrite [25]. These results can be explained on the basis of the electrical resistivity data of these samples. As discussed above, that the electrical resistivity initially decreases with the rise in temperature below the transition temperature and above the transition temperature, resistivity further decreases for aluminium substituted calcium hexaferrite. The initial increase in the drift mobility with increase in the temperature is due to the decrease in the electrical resistivity in this temperature range which causes to increase the mobility of the charge carriers. The increase in drift mobility above transition temperature is due to the fact that the electrical resistivity further decreases above this temperature and as a result the mobility of charge carriers increases rapidly.

IJARSCT
International Journal of Advanced Research in Science, Communication and Technology
International Open-Access, Double-Blind, Peer-Reviewed, Refereed, Multidisciplinary Online Journal
ISSN: 2581-9429
Volume 6, Issue 7, April 2026
Impact Factor: 8.2

IV. CONCLUSIONS

The aluminium doped calcium hexaferrites samples were synthesized by the microwave assisted sol-gel auto-combustion route. The XRD data have confirm the formation of M-type hexaferrites and the values of lattice parameters a and c of the sample supports this confirmation. The increase in temperature increases the electrical conductivity of the synthesized samples. An increase in electrical resistivity was noted with the substitution of Al^{3+} ions for Fe^{3+} ions, indicating the material's suitability for microwave device applications. Furthermore, the drift mobility was found to increase with higher aluminium concentration in the calcium hexaferrite system.

REFERENCES

[1] X. S. Liu, L. Fernandez Garcia, F. Hu, D. R. Zhu, M. Suárez, J. L. Menéndez, *Mater. Chem. Phys.* 133 (2012) 961–964.
[2] H. F. Yu, H. Y. Lin, *J. Magn. Magn. Mater*. 283 (2004) 190–198.
[3] Q. Q. Fang, H. W. Bao, D. M. Fang, J.Z. Wang, X. G. Li, *J. Magn. Magn. Mater*. 278 (2004) 122–126.
[4] D. Chen, Y. Liu, K. Yang and H. Zhang, *J. Magn. Magn. Mater*. 337 (2013) 65–69.
[5] N. Tran, H. S. Kim, T. L. Phan, D. S. Yang and B. W. Lee, *Ceram. Int.* 44 (2018) 12132.
[6] S. E. Shirsath, D. Wang, S. S. Jadhav, M. L. Mane and S. Li, Ferrites obtained by sol-gel method Handbook of Sol-Gel Science and Technology ed L Klein, M Aparicio and A Jitianu (Berlin: Springer) (2018) pp 695–735.
[7] M. A. Almessiere, Y. Slimani and A. Baykal, *Ceram. Int.* 45 (1) (2019) 963–969.
[8] M. N. Ashiq, M. J. Iqbal, M. N. Haq, P. H. Gomez and A. M. Qureshi, *J. Magn. Magn.Mater.* 324 (2012) 15–19
[9] A. Ataie, S. Heshmatimanesh and H. Kazempour, *J. Mater. Sci.* 37 (10) (2002) 2125–2128
[10] A. Sharma, O. Modi, G. Gupta, Adv. Appl. Sci. Research, 3 (4) (2012) 2151-2158.
[11] S. V. Bangale, D. R. Patil, S. R. Bamane, *Arch. Appl. Sci. Research*, 3 (5) (2011) 506-513.
[12] D. Lisjak, M. Drofenik, *J. Euro. Ceram. Soci*., 24 (2004) 1841-1845.
[13] S. R. Gawali and P. R. Moharkar, *Globle Journal of Engineering, Science and Social Science Studies* (ISSN No. 2394-3084),6(5) (2019) 11-15.
[14] S. Ounnunkad, P. Winotai, *J. Magn. Magn. Mater*. 301 (2006) 292-300.
[15] K. Haneda and H. Kojima, *Jap. J. Appl. Phys,* 12 (1973) 355.
[16] Sang Won Lee, Sung Yong An, In-Bo Shim, Chul Sung Kim, *J. Magn. Magn. Mater*. 290 (2005) 231-233.
[17] K. G. Rewatkar, N. M. Patil and S. R. Gawali, *Bull. Mater. Sci*., 28 (6) (2005) 585–587.
[18] D. K. Kulkarni, C. S. Prakash, *Bull. Mater. Sci*., 17 (1994) 35-39.
[19] C. Kittle, *An Introduction to Solid State Physics*, 5th ed.,Wiley, New York (1996).
[20] T. Abbas, M. U. Islam, M. A. Chaudhry, *Mod. Phys. Lett. B* 9 (22) (1995) 1419-1426.
[21] J. Smit, H. P. Wijn, *J. Ferrites Physical Properties of Ferrimagnetic Oxides in Relation to their Technical Applications*, John Wiley and Sons, New York, USA, (1959) 177-180.
[22] E. J. W. Verwey., De Boer J. H., Rec. Trans. Chem. Des. Pays. Bas. 55 (1936) 531.
[23] A. Lakshman, P. S. V. Subha Rao, B. P. Rao, K. H. Rao, *J. Phys. D. Appl. Phys*. 38 (2005) 673-678.
[24] Shahid Hussain, Asghari Maqsood, *Journal of Alloys and Compounds* Under Publication (2007).
[25] Muhammad Javed Iqbal, Muhammad Naeem Ashiq, Pablo Hernandez, *J. Phys.: Conf. Ser. (2009)*.